arXiv:submit/5682037 [cs.LG] 20 Jun 2024

Machine Learning Global Simulation of Nonlocal Gravity Wave Propagation

Aman Gupta [*1] **Aditi Sheshadri** [*1] **Sujit Roy** [*2] **Vishal Gaur** [2] **Manil Maskey** [3] **Rahul Ramachandran** [3]

Abstract

Global climate models typically operate at a grid resolution of hundreds of kilometers and fail to resolve atmospheric mesoscale processes, e.g., clouds, precipitation, and gravity waves (GWs). Model representation of these processes and their sources is essential to the global circulation and planetary energy budget, but subgrid scale contributions from these processes are often only approximately represented in models using *parameterizations*. These parameterizations are subject to approximations and idealizations, which limit their capability and accuracy. The most drastic of these approximations is the "single-column approximation" which completely neglects the horizontal evolution of these processes, resulting in key biases in current climate models. With a focus on atmospheric GWs, we present the first-ever global simulation of atmospheric GW fluxes using machine learning (ML) models trained on the WINDSET dataset to emulate global GW emulation in the atmosphere, as an alternative to traditional single-column parameterizations. Using an Attention U-Net-based architecture trained on globally resolved GW momentum fluxes, we illustrate the importance and effectiveness of global nonlocality, when simulating GWs using data-driven schemes.

1. Introduction

Gravity waves are fast-propagating perturbations in a stably stratified fluid. In the atmosphere, they are constantly generated by a myriad of sources like jet imbalance, geostrophic adjustment processes, flow over mountains, storm tracks, etc. Their spatial scales range from O(100) m to O(1000) km, i.e., they span across the atmospheric mesoscales and submesoscales.

Gravity waves (GWs) dynamically couple the different layers of the atmosphere and are among the key drivers of the meridional overturning circulation in the middle atmosphere (Fritts & Alexander, 2003; Achatz et al., 2023). They are primary contributors in driving the pole-to-pole mesospheric circulation (Holton, 1982; Becker, 2012). In the stratosphere, they influence the quasi-biennial oscillation (QBO) of tropical winds (Giorgetta et al., 2002), and the springtime breakdown of the Antarctic polar vortex (Gupta et al., 2021). GWs can also contribute to rapid breakdowns of the wintertime polar vortex, i.e., sudden warmings (Albers & Birner, 2014; Song et al., 2020), eventually influencing tropospheric storm tracks (Kidston et al., 2015; Domeisen & Butler, 2020).

Due to limited grid resolution, all state-of-the-art climate models represent subgrid momentum fluxes due to GWs using *parameterizations*. Depending on the source, these parameterizations can be broadly classified as orographic (for GWs generated over mountains, having zero ground-based phase speed) and nonorographic (generate elsewhere, having non-zero phase speeds). The most prominent orographic parameterizations include Lott & Miller (1997); van Niekerk et al. (2020) and the most prominent nonorographic parameterizations include Alexander & Dunkerton (1999); Scinocca (2002; 2003). All these schemes use the large-scale background state resolved by the climate models to predict the subgrid-scale momentum fluxes. The generated momentum fluxes are then coupled with the large-scale momentum equations that solve for the resolved flow dynamics in the model. Over nearly four decades now, all parameterizations have employed the single-column approximation, i.e., only the atmospheric state within a model vertical column is used to determine the GW flux in that column, thus neglecting any horizontal propagation that these waves exhibit. This assumption directly contradicts observations (Sato et al., 2009; 2012; Geldenhuys et al., 2023) and mesoscale resolving simulations (Kruse et al., 2022; Hindley et al., 2020; Gupta et al., 2024a), that show that GWs can often propagate horizontally thousands of kilometers away from their sources. Past studies have often reiterated the limitations of these assumptions and the urgent need to represent lateral propagation to resolve key circulation

[*]Equal contribution [1]Department of Earth System Science, Stanford University, Stanford, USA [2]Earth System Science Center, The University of Alabama in Huntsville, Huntsville, AL, USA [3]NASA Marshall Space Flight Center, Huntsville, AL, USA. Correspondence to: Aman Gupta <ag4680@stanford.edu>.

Proceedings of the 41st International Conference on Machine Learning, Vienna, Austria. PMLR 235, 2024. Copyright 2024 by the author(s).

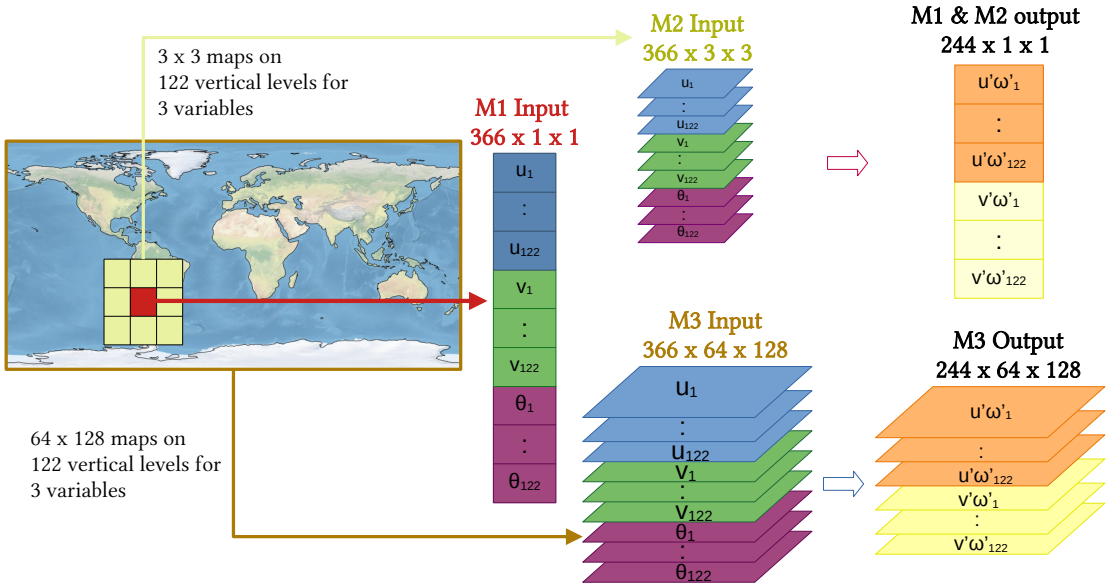

Figure 1. The three architectures used for global GW resolved momentum flux simulation. The three architectures, described in section 2.2 employ three different degrees of nonlocality. On one end, M1 uses single-column background data to predict the fluxes within that column. A timeslice is therefore a single vector of length 366. Intermediately, M2 uses background information in a 3×3 stencil to predict the fluxes within the single-column at the center of the stencil. A timeslice for M2 has dimensions $3 \times 3 \times 366$. On the other end, M3 uses global maps of the background field to predict global maps of fluxes. A timeslice for M3, thus, has dimensions $366 \times 64 \times 128$.

biases resulting from these assumptions (McLandress et al., 2012; de la Cámara et al., 2016; Kruse et al., 2022; Kim et al., 2024; Gupta et al., 2024b).

Although WKB ray-tracing-based (Amemiya & Sato, 2016; Voelker et al., 2023) and momentum redistribution-based schemes (Eichinger et al., 2023) provide viable alternatives to represent lateral propagation by simulating wave trajectories along which they conserve pseudomomentum, these schemes continue to face computational roadblocks.

Machine learning provides a promising, computationally efficient avenue to generate a new class of data-driven PDE solvers and model parameterizations that learn both large-scale and subgrid-scale physics, directly from high-quality data (Mansfield et al., 2023; Roy et al., 2024). Such ML schemes can be trained to take the background atmospheric state as input (just like traditional parameterizations) and use the state to predict the subgrid-scale momentum fluxes. These ML models can subsequently be coupled with the traditional Fortran-based momentum equations solvers. This effectively transforms the problem from the parameterization tuning and approximate modeling space into a problem that focuses on the development of physics-informed ML architectures and their optimal training on high-fidelity data.

This study focuses on the development of such parameterizations. Unlike existing models which have been trained on GW parameterization output, the goal here is to develop ML simulators that learn from inter-annual records of *resolved* momentum fluxes derived from modern reanalysis and kilometer-scale global climate models. The first step involves the training of ML models followed by offline testing of the inferred fluxes. The following step involves coupling these data-driven predictors to coarse-resolution models to test their online performance. Here, we focus on the first step.

The data-driven GW scheme discussed here is also being prepared to be used as part of a much larger foundation model for weather and climate, where it serves as a downstream application to first predict the global atmospheric state and then infer the small-scale GW flux distribution corresponding to that state.

1.1. Previous Works

ML emulation of gravity wave forcing in climate models has been explored in the past (Chantry et al., 2021; Espinosa et al., 2022; Lu et al., 2024; Sun et al., 2023). However, such efforts have focused on learning GW fluxes from parameterized drag, not resolved drag. Parameterized fluxes have highly analytical forms and contain biases. As a result, the ML models trained on such parameterizations, while easier to train, themselves contain these biases; pure-vertical GW

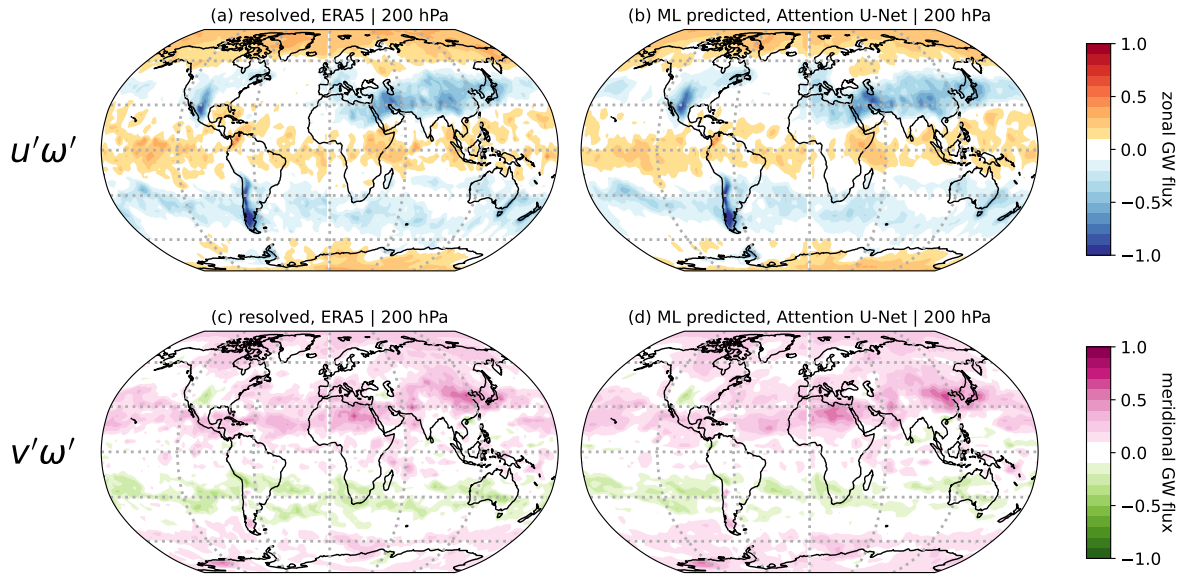

Figure 2. Mean predicted fluxes from globally nonlocal model, M3, for May 2015 at 200 hPa height. (a) and (b) respectively show the true mean and the predicted mean zonal flux ($u'\omega'$) for May 2015. (c) and (d) show the true mean and the predicted mean meridional flux ($v'\omega'$). The WINDSET dataset contains input variables and momentum fluxes which were normalized using a constant mean and standard deviation. Mean predicted fluxes for Models M1 and M3 are shown in Figures 4 and 5.

propagation being the most prominent bias.

Wang et al. (2022) proposed a strategy to embed nonlocality within ANNs by using input data from surrounding columns to infer the momentum fluxes within a given column. The strategy can be useful when learning from resolved GW momentum fluxes, as opposed to single-column output. This study, in part, builds upon their idea and explores different degrees of embedded spatial nonlocality: single-column, neighboring cells, and global nonlocality.

2. Methodology

2.1. Dataset

The training uses the "Weather Insights and Novel Data for Systematic Evaluation and Testing" (WINDSET) data introduced by Shinde et al. (2024). WINDSET is a compilation of multiple weather-related datasets incl. long-term precipitation forecasting, hurricane prediction and intensity estimation, aviation turbulence prediction, natural language forecasting, etc. It also comprises four years of the background field and resolved GW momentum fluxes derived from modern reanalysis, ERA5 (Hersbach et al., 2020).

The GW momentum fluxes in WINDSET used ERA5 at its native 30 km resolution to compute the background atmospheric state, and GW fluxes using Helmholtz decomposition, and conservatively coarsegrained the input fields and output fluxes to a 64 $\times$ 128 (latitude x longitude) Gaussian grid and 137 model levels. The 15 vertical levels near the model top are removed to eliminate artificial damping effects, and thus there are 122 vertical levels.

The input comprises the meteorological variables: zonal wind (u), meridional wind (v), potential temperature (θ). The vertical velocity (ω) is not added because the hydrostatic model allows only two degrees of freedom. θ serves as an appropriate vertical coordinate that combines both temperature and pressure information. The output comprises the zonal and meridional components of the vertical momentum flux ($u'\omega'$ and $v'\omega'$). The variables are stacked along the vertical dimension. Thus, an input timeslice has dimensions. 366 $\times$ 64 $\times$ 128 and an output timeslice has dimensions 244 $\times$ 64 $\times$ 128.

The data is available for four years: 2010, 2012, 2014, and 2015 at an hourly resolution. For single-column ANN training, this corresponds to $\approx$300 million data samples for training (not spatio-temporally uncorrelated). For global training, this corresponds to roughly 35k training samples.

2.2. Model Architecture

When dealing with nonlocal propagation of mesoscale systems, one pressing question arises naturally: *how much spatial nonlocality should the ML model represent?*. To address this, we train a set of three ML models which consider different degrees of nonlocality in their input:

M1. Single Column (1×1) ANN: with 4 hidden layers, each twice the input layer size (366), using ReLU activation, Adam optimized with cyclic learning rates. This single-column model aims to replicate the design for traditional single-column parameterizations.

M2. A nonlocal (3×3) ANN-CNN: that predicts the fluxes in a given column using the 3×3 grid surrounding the column. The first (input) layer is a 3×3 convolution layer which pools the data into a single column.

M3. Global Attention U-Net utilizing convolution layers (Oktay et al., 2018): that takes global (64×128) data with 366 input channels as input, encodes it using a U-Net backbone with residual connections scaled with attention multipliers, and decodes it to produce global flux predictions with 244 output channels.

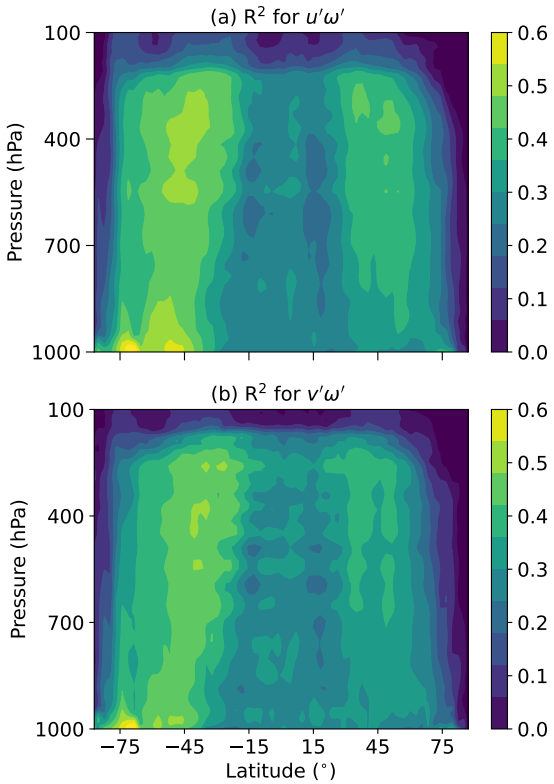

Figure 3. R^2 value for M3 for (a) zonal flux and (b) meridional flux predictions for May 2015. R^2 denotes the percent variance captured by the predictor. A higher R^2 value indicates better prediction.

The architectures are illustrated in Figure 1. The models were optimized to minimize the mean squared error. The models were trained on the four years of ERA5 data, except one month, May 2015, which was used for testing. Due to limited space, here, we discuss results only from the global nonlocal model (M3), which is the most complex among the three models considered.

3. Results

Predictions of the globally resolved fluxes using model M3 show a strong agreement, both in terms of the mean climatology for May 2015 (Figure 2) and intermediate snapshots (not shown). The predictions from M3 outperform predictions from both M1 and M2, demonstrating the importance of nonlocality and model complexity in learning the nonlinear evolution of atmospheric waves. The model accurately predicts both the structure and strength of the normalized fluxes over well-known stationary GW hotspots including the Rocky Mountains, the Andes, and the East Asian Mountains. Even in the tropics, where most GWs are generated by moist convective activity, the predicted mean climatology agrees reasonably well with the normalized fluxes from WINDSET (ERA5).

The prediction skill in the tropics is relatively weaker than in the midlatitudes, as quantified by the R^2 metric. For the zonal flux, M3 achieves an $R^2 \approx 0.6$ in the midlatitudes in both hemispheres. This value is down to 0.3-0.4 on average in the tropics. Moreover, the corresponding R^2 values are generally weaker for the meridional flux.

The prediction skill is quite poor in the stratosphere, where even negative R^2 values are obtained in the tropics. This is due to an exponential decrease in the background density and strong shear in the stratosphere, leading to data imbalance and reduced predictive skill. Efforts to enhance the prediction skill in the stratosphere are currently underway.

These results highlight (a) the challenges involved in simulating small-scale nonlocal wave evolution in the atmosphere, and (b) that simulation of non-stationary GWs can be more challenging than stationary or quasi-stationary GWs generated over orography which may have longer wavelengths.

This is work in progress and the next steps include transfer learning-focused experiments to combine the fluxes from WINDSET with GW fluxes obtained from global 1 km climate models that resolve the whole mesoscale spectrum.

Broader Impact

Model parameterizations present as a major source of uncertainty in current climate models. Success with nonlocal ML simulation of GWs can be extended to develop ML simulators for a broad range of unresolved mesoscale and submesoscale processes in coarse-climate models, potentially reducing model uncertainty.

These ML models can also be used as downstream plug-

ins for weather and climate foundation models for quick and inexpensive weather forecasting and climate prediction, empowering climate model use by the wider community and for educational purposes. Efforts in this direction are underway.

References

Achatz, U., Alexander, M. J., Becker, E., Chun, H.-Y., Dörnbrack, A., Holt, L., Plougonven, R., Polichtchouk, I., Sato, K., Sheshadri, A., Stephan, C. C., van Niekerk, A., and Wright, C. J. Atmospheric Gravity Waves: Processes and Parameterization. *Journal of the Atmospheric Sciences*, -1(aop), November 2023. ISSN 0022-4928, 1520-0469. doi: 10.1175/JAS-D-23-0210.1.

Albers, J. R. and Birner, T. Vortex Preconditioning due to Planetary and Gravity Waves prior to Sudden Stratospheric Warmings. *J. Atmos. Sci.*, 71(11):4028–4054, November 2014. ISSN 0022-4928, 1520-0469. doi: 10.1175/JAS-D-14-0026.1.

Alexander, M. J. and Dunkerton, T. J. A Spectral Parameterization of Mean-Flow Forcing due to Breaking Gravity Waves. *J. Atmos. Sci.*, 56(24):4167–4182, December 1999. ISSN 0022-4928. doi: 10.1175/1520-0469(1999)056⟨4167:ASPOMF⟩2.0.CO;2.

Amemiya, A. and Sato, K. A New Gravity Wave Parameterization Including Three-Dimensional Propagation. *Journal of the Meteorological Society of Japan. Ser. II*, 94(3): 237–256, 2016. doi: 10.2151/jmsj.2016-013.

Becker, E. Dynamical Control of the Middle Atmosphere. *Space Sci Rev*, 168(1):283–314, June 2012. ISSN 1572-9672. doi: 10.1007/s11214-011-9841-5.

Chantry, M., Hatfield, S., Dueben, P., Polichtchouk, I., and Palmer, T. Machine Learning Emulation of Gravity Wave Drag in Numerical Weather Forecasting. *Journal of Advances in Modeling Earth Systems*, 13(7): e2021MS002477, 2021. ISSN 1942-2466. doi: 10.1029/2021MS002477.

de la Cámara, A., Lott, F., Jewtoukoff, V., Plougonven, R., and Hertzog, A. On the Gravity Wave Forcing during the Southern Stratospheric Final Warming in LMDZ. *Journal of Atmospheric Sciences*, 73(8):3213–3226, August 2016. ISSN 0022-4928, 1520-0469. doi: 10.1175/JAS-D-15-0377.1.

Domeisen, D. I. V. and Butler, A. H. Stratospheric drivers of extreme events at the Earth's surface. *Commun Earth Environ*, 1(1):1–8, December 2020. ISSN 2662-4435. doi: 10.1038/s43247-020-00060-z.

Eichinger, R., Rhode, S., Garny, H., Preusse, P., Pisoft, P., Kuchař, A., Jöckel, P., Kerkweg, A., and Kern, B. Emulating lateral gravity wave propagation in a global chemistry–climate model (EMAC v2.55.2) through horizontal flux redistribution. *Geoscientific Model Development*, 16(19):5561–5583, October 2023. ISSN 1991-959X. doi: 10.5194/gmd-16-5561-2023.

Espinosa, Z. I., Sheshadri, A., Cain, G. R., Gerber, E. P., and DallaSanta, K. J. Machine Learning Gravity Wave Parameterization Generalizes to Capture the QBO and Response to Increased CO2. *Geophysical Research Letters*, 49(8):e2022GL098174, 2022. ISSN 1944-8007. doi: 10.1029/2022GL098174.

Fritts, D. C. and Alexander, M. J. Gravity wave dynamics and effects in the middle atmosphere. *Reviews of Geophysics*, 41(1), 2003. ISSN 1944-9208. doi: 10.1029/2001RG000106.

Geldenhuys, M., Kaifler, B., Preusse, P., Ungermann, J., Alexander, P., Krasauskas, L., Rhode, S., Woiwode, W., Ern, M., Rapp, M., and Riese, M. Observations of Gravity Wave Refraction and Its Causes and Consequences. *Journal of Geophysical Research: Atmospheres*, 128(3):e2022JD036830, 2023. ISSN 2169-8996. doi: 10.1029/2022JD036830.

Giorgetta, M. A., Manzini, E., and Roeckner, E. Forcing of the quasi-biennial oscillation from a broad spectrum of atmospheric waves. *Geophysical Research Letters*, 29 (8):86–1–86–4, 2002. ISSN 1944-8007. doi: 10.1029/2002GL014756.

Gupta, A., Birner, T., Dörnbrack, A., and Polichtchouk, I. Importance of Gravity Wave Forcing for Springtime Southern Polar Vortex Breakdown as Revealed by ERA5. *Geophysical Research Letters*, 48(10):e2021GL092762, 2021. ISSN 1944-8007. doi: 10.1029/2021GL092762.

Gupta, A., Reichert, R., Dörnbrack, A., Garny, H., Eichinger, R., Polichtchouk, I., Kaifler, B., and Birner, T. Estimates of Southern Hemispheric Gravity Wave Momentum Fluxes Across Observations, Reanalyses, and Kilometer-scale Numerical Weather Prediction Model. *Journal of the Atmospheric Sciences*, -1(aop), January 2024a. ISSN 0022-4928, 1520-0469. doi: 10.1175/JAS-D-23-0095.1.

Gupta, A., Sheshadri, A., Alexander, M. J., and Birner, T. Insights on Lateral Gravity Wave Propagation in the Extratropical Stratosphere from 44 Years of ERA5 Data. *Geophysical Research Letters*, 2024b. ISSN 1944-8007. doi: 10.1029/2024GL108541.

Hersbach, H., Bell, B., Berrisford, P., Hirahara, S., Horányi, A., Muñoz-Sabater, J., Nicolas, J., Peubey, C., Radu, R.,

Schepers, D., Simmons, A., Soci, C., Abdalla, S., Abellan, X., Balsamo, G., Bechtold, P., Biavati, G., Bidlot, J., Bonavita, M., Chiara, G. D., Dahlgren, P., Dee, D., Diamantakis, M., Dragani, R., Flemming, J., Forbes, R., Fuentes, M., Geer, A., Haimberger, L., Healy, S., Hogan, R. J., Hólm, E., Janisková, M., Keeley, S., Laloyaux, P., Lopez, P., Lupu, C., Radnoti, G., de Rosnay, P., Rozum, I., Vamborg, F., Villaume, S., and Thépaut, J.-N. The ERA5 global reanalysis. *Quarterly Journal of the Royal Meteorological Society*, 146(730):1999–2049, 2020. ISSN 1477-870X. doi: 10.1002/qj.3803.

Hindley, N. P., Wright, C. J., Hoffmann, L., Moffat-Griffin, T., and Mitchell, N. J. An 18-Year Climatology of Directional Stratospheric Gravity Wave Momentum Flux From 3-D Satellite Observations. *Geophysical Research Letters*, 47(22):e2020GL089557, 2020. ISSN 1944-8007. doi: 10.1029/2020GL089557.

Holton, J. R. The Role of Gravity Wave Induced Drag and Diffusion in the Momentum Budget of the Mesosphere. *Journal of the Atmospheric Sciences*, 39(4):791–799, April 1982. ISSN 0022-4928, 1520-0469. doi: 10.1175/1520-0469(1982)039⟨0791:TROGWI⟩2.0.CO;2.

Kidston, J., Scaife, A. A., Hardiman, S. C., Mitchell, D. M., Butchart, N., Baldwin, M. P., and Gray, L. J. Stratospheric influence on tropospheric jet streams, storm tracks and surface weather. *Nature Geosci*, 8(6):433–440, June 2015. ISSN 1752-0894, 1752-0908. doi: 10.1038/ngeo2424.

Kim, Y.-H., Voelker, G. S., Bölöni, G., Zängl, G., and Achatz, U. Crucial role of obliquely propagating gravity waves in the quasi-biennial oscillation dynamics. *Atmospheric Chemistry and Physics*, 24(5):3297–3308, March 2024. ISSN 1680-7316. doi: 10.5194/acp-24-3297-2024.

Kruse, C. G., Alexander, M. J., Hoffmann, L., van Niekerk, A., Polichtchouk, I., Bacmeister, J. T., Holt, L., Plougonven, R., Šácha, P., Wright, C., Sato, K., Shibuya, R., Gisinger, S., Ern, M., Meyer, C. I., and Stein, O. Observed and Modeled Mountain Waves from the Surface to the Mesosphere near the Drake Passage. *Journal of the Atmospheric Sciences*, 79(4):909–932, April 2022. ISSN 0022-4928, 1520-0469. doi: 10.1175/JAS-D-21-0252.1.

Lott, F. and Miller, M. J. A new subgrid-scale orographic drag parametrization: Its formulation and testing. *Quarterly Journal of the Royal Meteorological Society*, 123(537):101–127, 1997. ISSN 1477-870X. doi: 10.1002/qj.49712353704.

Lu, Y., Xu, X., Wang, L., Liu, Y., Wu, T., Jie, W., and Sun, J. Machine Learning Emulation of Subgrid-Scale Orographic Gravity Wave Drag in a General Circulation Model With Middle Atmosphere Extension. *Journal of Advances in Modeling Earth Systems*, 16 (3):e2023MS003611, 2024. ISSN 1942-2466. doi: 10.1029/2023MS003611.

Mansfield, L. A., Gupta, A., Burnett, A. C., Green, B., Wilka, C., and Sheshadri, A. Updates on Model Hierarchies for Understanding and Simulating the Climate System: A Focus on Data-Informed Methods and Climate Change Impacts. *Journal of Advances in Modeling Earth Systems*, 15(10):e2023MS003715, 2023. ISSN 1942-2466. doi: 10.1029/2023MS003715.

McLandress, C., Scinocca, J. F., Shepherd, T. G., Reader, M. C., and Manney, G. L. Dynamical Control of the Mesosphere by Orographic and Nonorographic Gravity Wave Drag during the Extended Northern Winters of 2006 and 2009. *J. Atmos. Sci.*, 70(7):2152–2169, December 2012. ISSN 0022-4928. doi: 10.1175/JAS-D-12-0297.1.

Oktay, O., Schlemper, J., Folgoc, L. L., Lee, M., Heinrich, M., Misawa, K., Mori, K., McDonagh, S., Hammerla, N. Y., Kainz, B., Glocker, B., and Rueckert, D. Attention U-Net: Learning Where to Look for the Pancreas, May 2018.

Roy, S., Leong, W. J., Shinde, R., Phillips, C. E., Kumar, A., Maskey, M., and Ramachandran, R. CLIFFORD NEURAL OPERATORS ON ATMOSPHERIC DATA INFLUENCED PARTIAL DIFFERENTIAL EQUATIONS. In *ICLR 2024 Workshop on AI4DifferentialEquations In Science*, March 2024.

Sato, K., Watanabe, S., Kawatani, Y., Tomikawa, Y., Miyazaki, K., and Takahashi, M. On the origins of mesospheric gravity waves. *Geophysical Research Letters*, 36(19), 2009. ISSN 1944-8007. doi: 10.1029/2009GL039908.

Sato, K., Tateno, S., Watanabe, S., and Kawatani, Y. Gravity Wave Characteristics in the Southern Hemisphere Revealed by a High-Resolution Middle-Atmosphere General Circulation Model. *Journal of Atmospheric Sciences*, 69 (4):1378–1396, April 2012. ISSN 0022-4928, 1520-0469. doi: 10.1175/JAS-D-11-0101.1.

Scinocca, J. F. The Effect of Back-Reflection in the Parameterization of Non-Orographic Gravity-Wave Drag. *Journal of the Meteorological Society of Japan. Ser. II*, 80(4B):939–962, 2002. doi: 10.2151/jmsj.80.939.

Scinocca, J. F. An Accurate Spectral Nonorographic Gravity Wave Drag Parameterization for General Circulation Models. *Journal of Atmospheric Sciences*, 60(4): 667–682, February 2003. ISSN 0022-4928, 1520-0469. doi: 10.1175/1520-0469(2003)060⟨0667:AASNGW⟩2.0.CO;2.

Shinde, R., Phillips, C. E., Roy, S., Gupta, A., Sheshadri, A., Maskey, M., and Ramachandran, R. WINDSET: Weather Insights and Novel Data for Systematic Evaluation and Testing. In *ICLR 2024 Workshop on Data-centric Machine Learning Research (DMLR): Harnessing Momentum for Science*, May 2024.

Song, B.-G., Chun, H.-Y., and Song, I.-S. Role of Gravity Waves in a Vortex-Split Sudden Stratospheric Warming in January 2009. *Journal of the Atmospheric Sciences*, 77(10):3321–3342, September 2020. ISSN 0022-4928, 1520-0469. doi: 10.1175/JAS-D-20-0039.1.

Sun, Y. Q., Hassanzadeh, P., Alexander, M. J., and Kruse, C. G. Quantifying 3D Gravity Wave Drag in a Library of Tropical Convection-Permitting Simulations for Data-Driven Parameterizations. *Journal of Advances in Modeling Earth Systems*, 15(5):e2022MS003585, 2023. ISSN 1942-2466. doi: 10.1029/2022MS003585.

van Niekerk, A., Sandu, I., Zadra, A., Bazile, E., Kanehama, T., Köhler, M., Koo, M.-S., Choi, H.-J., Kuroki, Y., Toy, M. D., Vosper, S. B., and Yudin, V. COnstraining ORographic Drag Effects (COORDE): A Model Comparison of Resolved and Parametrized Orographic Drag. *Journal of Advances in Modeling Earth Systems*, 12(11):e2020MS002160, 2020. ISSN 1942-2466. doi: 10.1029/2020MS002160.

Voelker, G. S., Bölöni, G., Kim, Y.-H., Zängl, G., and Achatz, U. MS-GWaM: A 3-dimensional transient gravity wave parametrization for atmospheric models, September 2023.

Wang, P., Yuval, J., and O'Gorman, P. A. Non-Local Parameterization of Atmospheric Subgrid Processes With Neural Networks. *Journal of Advances in Modeling Earth Systems*, 14(10):e2022MS002984, 2022. ISSN 1942-2466. doi: 10.1029/2022MS002984.

4. Appendix

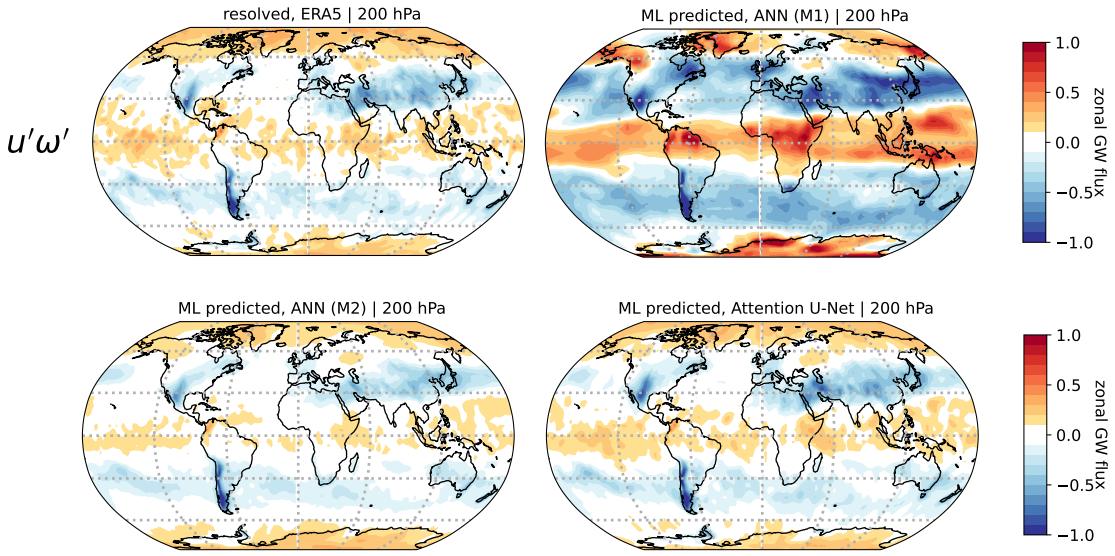

Figure 4. Mean predicted fluxes compared with the (top left) true ERA5 flux from the (top right) M1: single-column ANN, (bottom left) M2: 3x3 nonlocal columns ANN, and (bottom right) M3: globally nonlocal Attnetion U-Net CNN, for May 2015 at 200 hPa height. The figure compares the true mean and the predicted mean vertical flux of zonal momentum ($u'\omega'$) for the 3 models trained for the same number of epochs. The 1x1 and 3x3 ANNs had identical hyperparameters and the 3x3 input was processed and propagated into a single 1x1 column input by applying a 3x3 2D convolution layer. Even though the 1x1 ANN roughly captures the gross structure of the fluxes, and identifies the stationary hotspots in the midlatitudes to a certain degree, the predictions have a clear strong bias. Moreover, M1 incorrectly predicts the sign of the zonal flux over most of the Northern polar region and the sign of the meridional flux over most of the Southern polar region. Introducing nonlocal leads to a drastic improvement in performance, reduced model overfitting, and produces better prediction. The globally nonlocal UNet provides the best prediction.

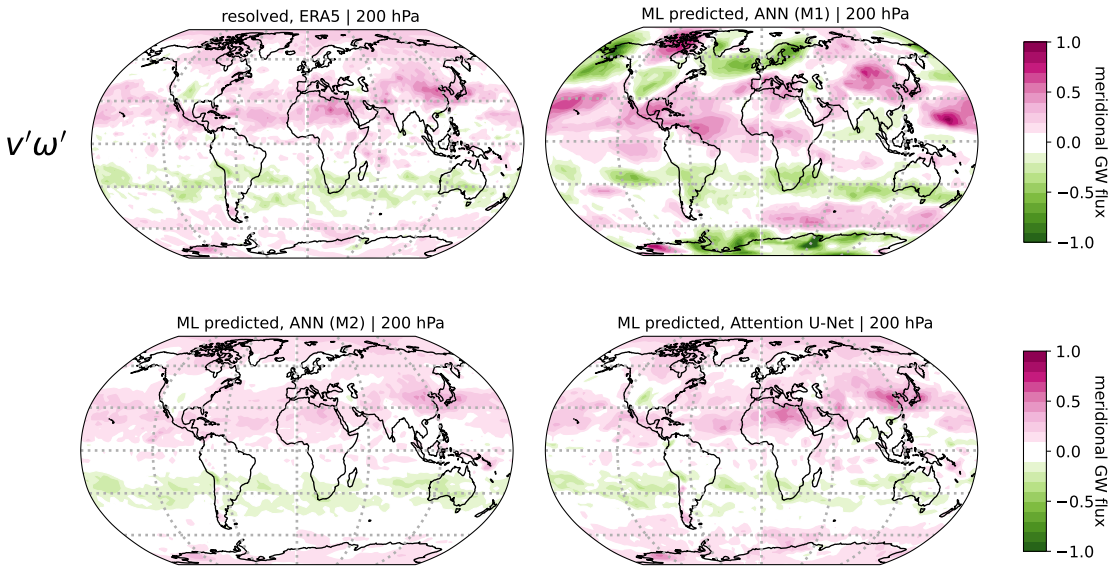

Figure 5. Same comparison as in Figure 5, but for the meridional flux of vertical momentum ($v'\omega'$) at 200 hPa.

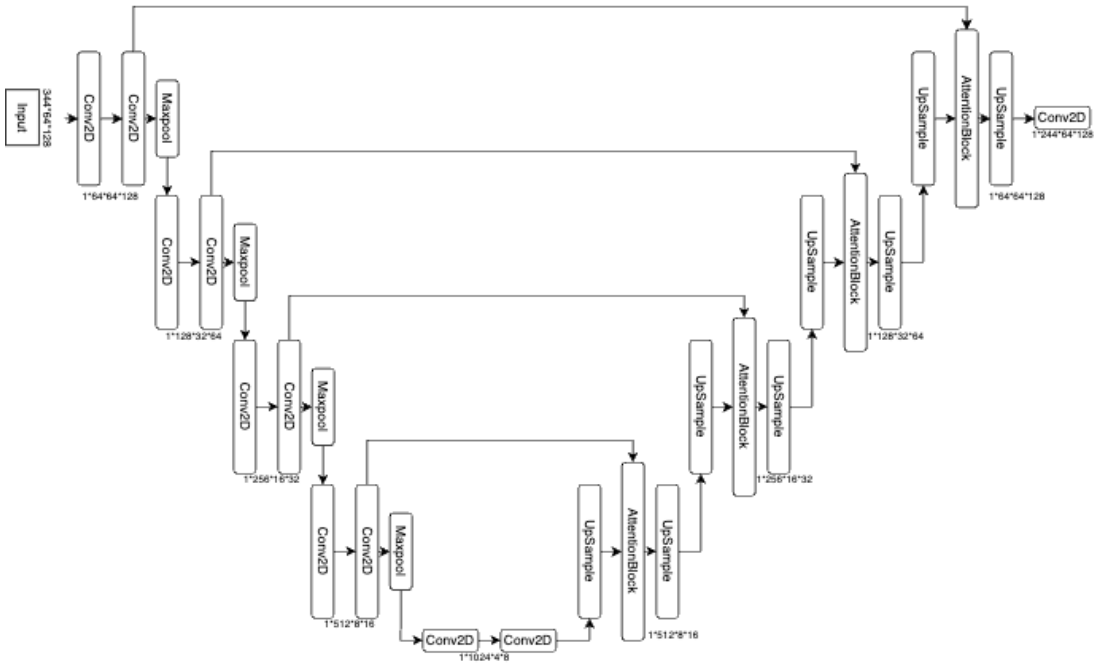

Figure 6. Schematic illustrating the architecture of the Attention-UNET used in the global nonlocal model M3.

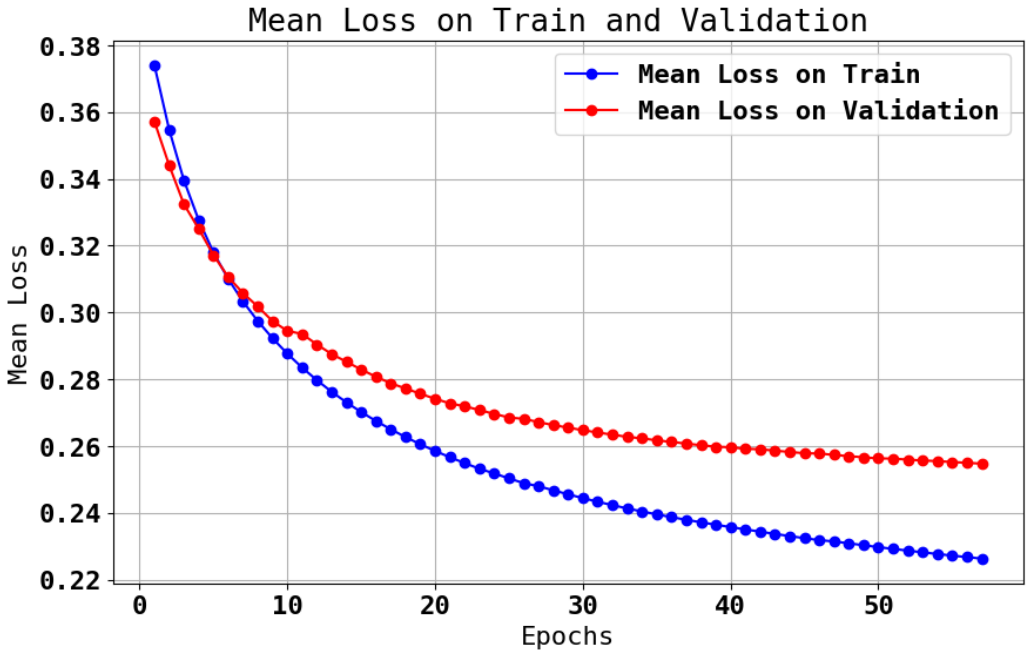

Figure 7. Training and Validation loss curve for the Attention-UNet model, M3.